Neurochemistry International 63 (2013) 423–431

Contents lists available at ScienceDirect

Neurochemistry International

journal homepage: www.elsevier.com/locate/nci

(−)-Reboxetine inhibits muscle nicotinic acetylcholine receptors by interacting with luminal and non-luminal sites

Hugo R. Arias [a,*], Marcelo O. Ortells [b], Dominik Feuerbach [c]

[a] Department of Medical Education, California Northstate University College of Medicine, Elk Grove, CA, USA
[b] Faculty of Medicine and CONICET, University of Morón, Argentina
[c] Novartis Institutes for Biomedical Research, Basel, Switzerland

ARTICLE INFO

Article history:
Received 29 May 2013
Received in revised form 23 July 2013
Accepted 25 July 2013
Available online 31 July 2013

Keywords:
Nicotinic acetylcholine receptors
Conformational states
Antidepressants
Norepinephrine selective reuptake inhibitor
Reboxetine

ABSTRACT

The interaction of (−)-reboxetine, a non-tricyclic norepinephrine selective reuptake inhibitor, with muscle-type nicotinic acetylcholine receptors (AChRs) in different conformational states was studied by functional and structural approaches. The results established that (−)-reboxetine: (a) inhibits (±)-epibatidine-induced Ca^{2+} influx in human (h) muscle embryonic (hα1β1γδ) and adult (hα1β1εδ) AChRs in a non-competitive manner and with potencies IC_{50} = 3.86 ± 0.49 and 1.92 ± 0.48 μM, respectively, (b) binds to the [^{3}H]TCP site with ~13-fold higher affinity when the *Torpedo* AChR is in the desensitized state compared to the resting state, (c) enhances [^{3}H]cytisine binding to the resting but activatable*Torpedo* AChR but not to the desensitized AChR, suggesting desensitizing properties, (d) overlaps the PCP luminal site located between rings 6′ and 13′ in the *Torpedo* but not human muscle AChRs. *In silico* mutation results indicate that ring 9′ is the minimum structural component for (−)-reboxetine binding, and (e) interacts to non-luminal sites located within the transmembrane segments from the *Torpedo* AChR γ subunit, and at the α1/ε transmembrane interface from the adult muscle AChR. In conclusion, (−)-reboxetine non-competitively inhibits muscle AChRs by binding to the TCP luminal site and by inducing receptor desensitization (maybe by interacting with non-luminal sites), a mechanism that is shared by tricyclic antidepressants.

1. Introduction

(±)-Reboxetine is a non-tricyclic norepinephrine selective reuptake inhibitor (NSRI) that inhibits neuronal nicotinic acetylcholine receptors (AChRs) (Arias et al., 2013; Miller et al., 2002; reviewed in Arias et al. (2006)). Additional studies also support a link between AChRs and the pharmacological activity of reboxetine. For example, animal behavior results indicate that nicotinic agonists enhance the antidepressant activity elicited by reboxetine (Andreasen and Redrobe, 2009; Andreasen et al., 2011), and that reboxetine attenuates nicotine self-administration in rats (Rauhut et al., 2002). Considering these results, neuronal AChRs can be targets for the beneficial action elicited by reboxetine.

From the mechanistic point of view, (−)-reboxetine inhibits noncompetitively human (h) α4β2 AChRs mainly by an open channel blocking mechanism (Arias et al., 2013). This inhibition is mediated by interacting with a luminal site located in the middle of the ion channel and with an intrasubunit site located within the α4 transmembrane segments. Although we have a better understanding of the inhibitory process at hα4β2 AChRs, we do not know the structural components of the binding sites and the inhibitory mechanisms of (−)-reboxetine at other AChR subtypes. In this regard, we will take advantage of the natural mutations between the hα4β2 and muscle AChRs, including *Torpedo* AChRs (i.e., Tα1β1γδ) as well as human adult (i.e., hα1β1εδ) and embryonic (i.e., hα1β1γδ) muscle AChRs, to advance in the pharmacological and structural characterization of the interaction of (−)-reboxetine with distinctAChRs. An advantage of using muscle AChRs is that the interaction of the phencyclidine (PCP) analog [^{3}H]TCP {[piperidyl-3, 4-^{3}H(*N*)]-*N*-(1-(2 thienyl)cyclohexyl)-3, 4-piperidine)} has been previously characterized in these AChRs, especially in *Torpedo* AChRs (reviewed in Arias et al. (2006)).

Abbreviations: AChR, nicotinic acetylcholine receptor; NSRI, norepinephrine selective reuptake inhibitor; TCAs, tricyclic antidepressants; NCA, non-competitive antagonist; (−)-reboxetine, (−)-*R,R*-([2-[α[2-ethoxyphenoxy]benzyl]-morpholine); PCP, phencyclidine; [^{3}H]TCP, piperidyl-3, 4-3H(*N*)]-(*N*-(1-(2 thienyl)cyclohexyl)-3, 4-piperidine; CCh, carbamylcholine; α-BTx, α-bungarotoxin; RT, room temperature; BS, binding saline; K_i, inhibition constant; IC_{50}, ligand concentration that inhibits 50% binding or ion flux; EC_{50}, ligand concentration that produces 50% increase of binding; n_H, Hill coefficient; DMEM, dulbecco's modified eagle medium; FBS, fetal bovine serum; RMSD, root mean square deviation.

* Corresponding author. Address: Department of Medical Education, California Northstate University College of Medicine, 9700W. Taron Dr., Elk Grove, CA 95757, USA. Tel.: +1 (916) 686 7300; fax: +1 (916) 686 7310.
E-mail address: hugo.arias@cnucom.org (H.R. Arias).

0197-0186/$ - see front matter © 2013 Elsevier Ltd. All rights reserved.
http://dx.doi.org/10.1016/j.neuint.2013.07.009

Since the inhibitory action of reboxetine on AChRs might be relevant for its pharmacological actions (Andreasen and Redrobe, 2009; Andreasen et al., 2011; Rauhut et al., 2002), the interaction of this non-tricyclic NSRI with several muscle AChR subtypes in different conformational states is characterized and subsequently compared to that for the hα4β2 AChR (Arias et al., 2013). To accomplish these objectives, several approaches are used, including [^{3}H]TCP and [^{3}H]cytisine competition binding, Ca^{2+} influx, molecular docking, molecular dynamics, and *in silico* mutations.

2. Materials and methods

2.1. Materials

[^{3}H]TCP ([piperidyl-3, 4-^{3}H(*N*)]-(*N*-(1-(2 thienyl)cyclohexyl)-3, 4-piperidine) (45 Ci/mmol), and [^{3}H]cytisine hydrochloride (35.6 Ci/mmol) were obtained from PerkinElmer Life Sciences Products, Inc. (Boston, MA, USA), and stored at −20 °C. Phencyclidine hydrochloride (PCP) was obtained through the National Institute on Drug Abuse (NIDA) (NIH, Baltimore, MA, USA). (−)-Reboxetine mesylate, carbamylcholine chloride (CCh), proadifen hydrochloride, were purchased from Sigma–Aldrich (St. Louis, MO, USA). (±)-Epibatidine hydrochloride was obtained from Tocris Bioscience (Ellisville, MO, USA). α-Bungarotoxin (α-BTx) was purchased from Invitrogen Co. (Carlsbad, CA, USA). Fetal bovine serum (FBS) and trypsin/EDTA were purchased from Gibco BRL (Paisley, UK). Salts were of analytical grade.

2.2. Ca^{2+} influx measurements in TE671-hα1β1γδ and HAM293-hα1β1δ cells

Ca^{2+} influx was determined as previously described (Arias et al., 2009, 2010a; Michelmore et al., 2002). Briefly, TE671-hα1β1γδ and HAM293-hα1β1εδ cells were seeded 48 h prior to the experiment on black 96-well plates (Costar, New York, USA) in medium consisting of DMEM/10% FBS at a density of 5×10^4 cells per well and incubated at 37°C in a humidified atmosphere (5% CO_2/95% air). On the day of the experiment, the medium was removed by flicking the plates and replaced with 100 μL DMEM/10% FBS containing 2 μM Fluo-4 (Molecular Probes, Eugene, Oregon, USA) in the presence of 2.5 mM probenecid (Sigma, Buchs, Switzerland). The cells were then incubated at 37 °C in a humidified atmosphere (5% CO_2/95% air) for 1 h. Plates were flicked to remove excess of Fluo-4, washed once with HBSS/NMDG buffer (130 mM N-methyl-D-glucamine, 4.5 mM KCl, 2 mM $CaCl_2$, 0.8 mM $MgSO_4$, 0.9 mM KH_2PO_4, 25 mM glucose, 20 mM HEPES, pH 7.4), and finally refilled with 100 μL of HBSS/NMDG containing different concentrations of (−)-reboxetine and incubated for 5 min at RT. Plates were then placed in the cell plate stage of the fluorimetric imaging plate reader (Molecular Devices, Sunnyvale, CA, USA). A baseline consisting of five measurements of 0.4 s each was recorded. (±)-Epibatidine (1 μM) was then added from the agonist plate to the cell plate using the 96-tip pipettor simultaneously to fluorescence recordings for a total length of 3 min. The laser excitation and emission wavelengths are 488 and 510 nm, at 1 W, with a CCD camera opening of 0.4 s.

2.3. Radioligand binding experiments using Torpedo AChRs in different conformational states

The effect of (−)-reboxetine on [^{3}H]TCP binding to *Torpedo* AChRs in the resting and desensitized was studied as previously described (Arias et al., 2003, 2009, 2010a; Sanghvi et al., 2008). In this regard, *Torpedo* AChR native membranes (0.3 μM) were suspended in binding saline (BS) buffer (50 mM Tris–HCl, 120 mM NaCl, 5 mM KCl, 2 mM $CaCl_2$, 1 mM $MgCl_2$, pH 7.4) with 6.5 nM [^{3}H]TCP in the presence of 1 mM CCh (desensitized/CCh-bound state), or alternatively with 9.2 nM [^{3}H]TCP in the presence of 1 μM α-BTx (resting/α-BTx-bound state; (Moore and McCarthy, 2012)), and preincubated for 30 min at room temperature (RT). Nonspecific binding was determined in the presence of 50 (desensitized experiments) or 100 μM PCP (resting experiments).

To determine whether (−)-reboxetine modulates agonist binding to AChRs in different conformational states, *Torpedo* AChR membranes (0.3 μM) were incubated with 7.7 nM [^{3}H]cytisine in the absence (resting but activatable state) or in the presence of 200 μM proadifen (desensitized/proadifen-bound state; Arcava and Albuquerque, 1984). The nonspecific binding was determined in the presence 1 mM CCh.

The total volume was divided into aliquots, and increasing concentrations of (−)-reboxetine were added to each tube and incubated for 2 h at RT. AChR-bound radioligand was then separated from free ligand by a filtration assay using a 48-sample harvester system with GF/B Whatman filters (Brandel Inc., Gaithersburg, MD, USA), previously soaked with 0.5% polyethylenimine for 30 min. The membrane-containing filters were transferred to scintillation vials with 3 mL of Bio-Safe II (Research Product International Corp, Mount Prospect, IL, USA), and the radioactivity was determined using a Beckman LS6500 scintillation counter (Beckman Coulter, Inc., Fullerton, CA, USA). The concentration–response data were curve-fitted by nonlinear least squares analysis using the Prism software (GraphPad Software, San Diego, CA). The observed IC_{50} values from the competition experiments described above were transformedinto inhibition constant (K_i) values using the Cheng–Prusoff relationship (Cheng and Prusoff, 1973):

$$K_i = IC_{50}/1 + ([[^3\text{H}]\text{TCP}]/K_d^{\text{TCP}}) \quad (1)$$

where [[^{3}H]TCP] is the initial concentration of [^{3}H]TCP, and K_d^{TCP} corresponds to the dissociation constant for [^{3}H]TCP in the resting (0.83 μM; Arias et al., 2003) and desensitized (0.25 μM; Pagán et al., 2001) *Torpedo* AChRs, respectively. The K_i and n_H values were summarized in Table 2.

2.4. Molecular docking and molecular dynamics simulations of (−)-reboxetine in muscle AChRs

The electron microscopy structure of the *Torpedo* AChR determined at a resolution of ~4 Å (PDB 2BG9) (Miyazawa et al., 2003; Unwin, 2005) was used as a template for the construction of the *Torpedo* AChR model. The*Torpedo* AChR structure (i.e., α1β1γδ) was energy minimized using molecular mechanics (Keserü and Kolossváry, 1999) in two steps, using the program NAMD (Phillips et al., 2005), the CHARMM force field (Brooks et al., 1983), and the software VEGA ZZ as interface (Pedretti et al., 2004). The energy minimization was carried out fixing the backbone atoms to their original positions, to avoid distorting the secondary structure. The human adult muscle AChR model (i.e., hα1β1εδ) was built by homology modeling also using the structure of the *Torpedo* AChR as the template by employing the programs Modeller 9.8 (Šali and Blundell, 1993) and SWIFT MODELLER (Mathur and Shankaracharya Vidyarthi, 2011). The model was minimized following the same protocol employed for the *Torpedo* AChR.

(−)-Reboxetine, in the protonated and neutral states, was first modeled using the VEGA ZZ program (Pedretti et al., 2004). Minimization and partial charge calculations were performed using the MOPAC program as implemented in VEGA ZZ and employing the semiempirical AM1 method.

The automatic docking procedure employed to investigate the binding modes of (−)-reboxetine in the AChR models was the implemented in the AutoDock Vina program (version 1.1.1) (Trott

and Olson, 2010). The complete AChR structure was used as the target for the simulated docking experiments thus avoiding restricting the binding sites to a particular region of the receptor. The parameters used were exhaustiveness = 570 and maximum number of modes = 20. Although the default and recommended value for the exhaustiveness parameter is 8, we employed the maximum value our computational system (an AMD X6 six core processor computer with 8 Gb RAM) allowed. No flexible residues were allowed in the transmembrane domain models to reduce computational time.

The program gives the best 20 poses found for each run, after performing an internal "clustering" that trimmers similar results. Nevertheless, several of the best 20 conformers are still superposed. From every cluster of superposed conformations, we selected the one with the best energy of binding. In this way, the number of binding sites found in every run is defined by the number of conformers remaining after this selection process.

To test the stability of (−)-reboxetine within their predicted docking sites, 10-ns or 20-ns molecular dynamics simulations were performed at 300 K using the program NAMD, CHARMM force field, and the software VEGA ZZ as interface. For this purpose, AChR models were hydrated with a 10 Å minimum thick shell using the program solvate 1.0 (Grubmueller, 1996), and the system was fully minimized using NAMD. To reduce computation time all residues and water molecules outside a 30 Å radius sphere and centered on the corresponding conformer were restricted to their original positions whilst those within this sphere were free to move. The same size sphere was used to implement a spherical periodic boundary condition.

The root mean square deviation (RMSD) values with respect to the initial structure (i.e., inter-molecular conformational changes, and the rotation and translation of the whole molecule), were extracted every 10-ps from the simulation (e.g., 10–20 ns) using the program VEGA ZZ (see Arias et al. (2013), for more details).

3. Results

3.1. (−)-Reboxetine-induced inhibition of (±)-epibatidine-mediated Ca^{2+} influx in TE671-hα1β1γδ and HAM293-hα1β1εδ cells

The potency of (±)-epibatidine to activate muscle AChRs was first determined by assessing the fluorescence change in TE671-hα1β1γδ (Fig. 1A) and HAM293-hα1β1εδ (Fig. 1B) cells, respectively, caused by an increase in intracellular Ca^{2+} after agonist stimulation. Increased concentrations of (±)-epibatidine activate the AChRs with potency EC_{50} = 0.26 ± 0.04 (hα1β1γδ) and 0.64 ± 0.06 μM (hα1β1εδ), respectively. The observed potencies for muscle AChRs are in the same concentration range as those previously determined (Arias et al., 2009, 2010a; Michelmore et al., 2002). The fact that the n_H value of (±)-epibatidine for the hα1β1εδ AChR is higher than unity (Table 1) indicates that the stimulatory process is produced in a cooperative manner.

(±)-Epibatidine-induced AChR activation is blocked by pre-incubation with (−)-reboxetine (Fig. 1A and B), with inhibitory potency IC_{50} = 3.86 ± 0.49 (hα1β1γδ) and 1.92 ± 0.48 μM (hα1β1εδ), respectively (see Table 1). These values indicate that (−)-reboxetine is more potent in human muscle AChRs compared to the hα4β2 AChR (Arias et al., 2013). Since the plasma concentration of reboxetine in patients under chronic treatment (6 months) is ~0.7 μM (Öhman et al., 2003), the observed inhibitory potency would produce minor effects, if any, on muscle AChRs from adults and embryos. This is in accord with the fact that reboxetine does not produce any side effects related with muscle weakness.

The fact that the n_H values for (−)-reboxetine are slightly higher than unity (Table 1), suggests that the inhibitory process is produced in a cooperative manner or by different mechanisms. To determine the mechanism of inhibition elicited by (−)-reboxetine on muscle AChRs, different concentrations of (−)-reboxetine were challenged against one (±)-epibatidine concentration on the

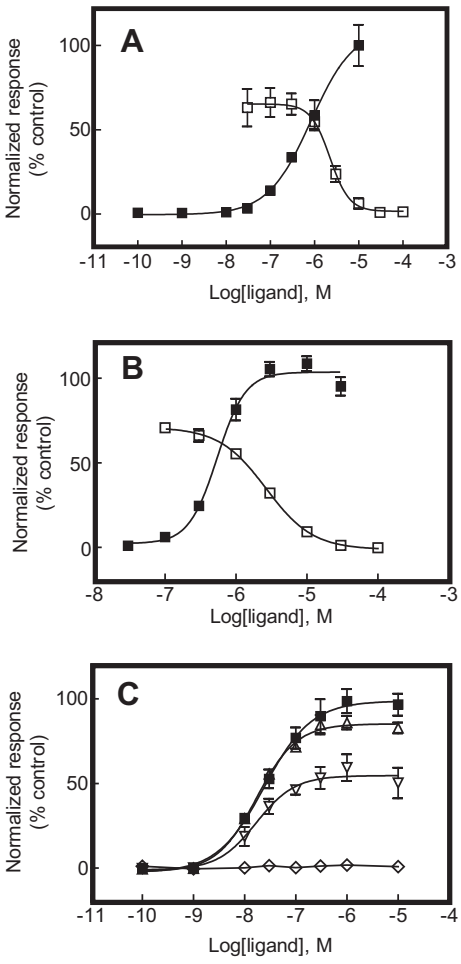

Fig. 1. (−)-Reboxetine-induced inhibition of (±)-epibatidine-evoked calcium influx in (A) TE671-hα1β1γδ and (B) HAM293-hα1β1εδ cells. Increased concentrations of (±)-epibatidine (■) activate the human (A) embryonic and (B) adult muscle AChRs with different potencies. Subsequently, cells were pre-treated with several concentrations of (−)-reboxetine (□), followed by addition of 1.0 μM (±)-epibatidine. Response was normalized to the maximal (±)-epibatidine response which was set as 100%. (C) Pre-treatment with 1 (Δ), 3 (▽), or 30 μM (−)-reboxetine (◇) (n = 6) inhibits (±)-epibatidine-elicited hα1β1γδ AChR activation (■) in a dose dependent and noncompetitive manner. The plots are representative of 27 (A; ■), 13 (B; ■), and 6 (A and B, □) determinations, respectively, where the error bars represent the standard deviations (S.D.). The EC_{50}, IC_{50}, and n_H values were obtained by nonlinear least-squares fit and summarized in Table 1.

Table 1
Activation potency (EC_{50}) of (±)-epibatidine and inhibitory potency (IC_{50}) of (−)-reboxetine for human muscle AChR subtypes obtained by Ca^{2+} influx measurements.

AChR subtype	EC_{50}, μM[a]	n_H[b]	IC_{50}, μM[a]	n_H[b]
hα1β1γδ (embryonic)	0.26 ± 0.04 (n = 27)	1.23 ± 0.06	3.86 ± 0.49 (n = 6)	1.35 ± 0.16
hα1β1εδ (adult)	0.64 ± 0.06 (n = 13)	2.01 ± 0.09	1.92 ± 0.48 (n = 6)	1.29 ± 0.12

n = number of experiments.
[a] Values were obtained from Fig. 1A (hα1β1γδ) and 1B (hα1β1εδ), respectively.
[b] Hill coefficients.

hα1β1γδ AChR (Fig. 1C). Since increasing (−)-reboxetine concentrations did not cause a rightward shift of the (±)-epibatidine curve and the maximal response of the agonist was not affected, the results indicate that (−)-reboxetine inhibits muscle AChRs by a non-competitive mechanism.

3.2. Radioligand binding experiments using Torpedo AChRs in different conformational states

Since (−)-reboxetine inhibits muscle AChRs by a noncompetitive mechanism, and considering that a noncompetitive inhibition can be produced by a luminal interaction, the effect of (−)-reboxetine on [^{3}H]TCP binding to *Torpedo* AChRs in different conformational states was studied. The results show that (−)-reboxetine inhibits ∼100% the specific binding of [^{3}H]TCP to the resting/α-BTx-bound and desensitized/CCh-bound AChRs (Fig. 2). Comparing the K_i values in different conformational states (Table 2), (−)-reboxetine binds to the [^{3}H]TCP site at the desensitized AChR with ∼13-fold higher affinity than that in the resting AChR. The fact that the calculatedn_H values for (−)-reboxetine are close to unity (Table 2) indicates that (−)-reboxetine inhibits [^{3}H]TCP binding in a non-cooperative manner. In turn, this result suggests that (−)-reboxetine may interact with a single binding site, probably inhibiting radioligand binding in a steric fashion.

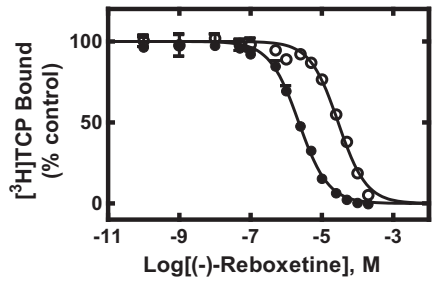

Fig. 2. (−)-Reboxetine-induced inhibition of [^{3}H]TCP binding to *Torpedo* AChRs in different conformational states. *Torpedo* AChR membranes (0.3 μM) were equilibrated (2 h) with 6.5 nM [^{3}H]TCP in the presence of 1 mM CCh (●) (desensitized/CCh-bound state), or with 9.2 nM [^{3}H]TCP in the presence of 1 μM α-BTx (○) (resting/α-BTx-bound state), and increasing concentrations of (−)-reboxetine. Nonspecific binding was determined in the presence of 50 (●) or 100 μM PCP (○). Each plot is the combination of three separated experiments each one performed in triplicate, where the error bars represents the S.D. values. From these plots the IC_{50} and $n_H$values were obtained by nonlinear least-squares fit. Subsequently, the K_i values were calculated using Eq. (1). The calculated K_i and n_H values are summarized in Table 2.

To determine additional mechanisms of inhibition elicited by (−)-reboxetine (e.g., ligand-induced desensitization), the effect of this NSRI on the binding of the agonist [^{3}H]cytisine to *Torpedo* AChRs in distinct conformational states was compared to that for tricyclic antidepressants (TCAs), including imipramine, amitriptyline, and doxepin. Fig. 3 shows that (−)-reboxetine and TCAs enhance [^{3}H]cytisine binding to *Torpedo* AChRs in the resting but activatable state (i.e., in the absence of proadifen). A potential explanation for this pharmacological effect is based on the fact that the AChR membrane suspension contains an excess of agonist binding sites (0.6 μM) compared with the initial concentration of [^{3}H]cytisine (7.7 nM). Since the cytisine K_i in the resting state is 1.6 μM (Arias et al., 2010a), only a small fraction of AChRs will be initially labeled with [^{3}H]cytisine. Considering $n_H = 1$, a fractional occupancy of ∼0.005% for [^{3}H]cytisine bound to the resting AChR is calculated. Thus, if the AChR is shifted to its high affinity state (i.e., the desensitized state), an increase in the AChR-bound [^{3}H]cytisine fraction can be expected. In this regard, considering that the cytisine K_i in the desensitized state is 0.45 μM (Arias et al., 2010a), a fractional occupancy of ∼0.017% for [^{3}H]cytisine bound to the desensitized AChR is obtained. This is an increase of ∼3-fold in fractional occupancy. Coincident with this calculation, our binding results indicate an increase of ∼2–4 times (see Fig. 3). The explanation of our results is that when the antidepressant binds to its site(s), the AChR becomes desensitized, the affinity of [^{3}H]cytisine is increased and subsequently, a larger fraction of AChR-bound [^{3}H]cytisine is observed. In order to quantify this enhanced binding, the drug concentration to produce 50% increase of [^{3}H]cytisine binding was calculated (i.e., Apparent EC_{50}s in Table 2). These values indicate that (−)-reboxetine and TCAs enhance [^{3}H]cytisine binding with the following desensitizing potency sequence (ApparentEC_{50} in μM): imipramine (1.2) > (−)-reboxetine (1.7) > doxepin (1.8) > amitriptyline (2.8).

Fig. 3 also shows that (−)-reboxetine and TCAs do not further enhance [^{3}H]cytisine binding to the already desensitized AChR (i.e., in the presence of 200 μM proadifen). This indicates that NSRIs and TCAs do not induce any additional conformational change in the already desensitized AChR (i.e., at maximal [^{3}H]cytisine binding). Moreover, TCAs, but not (−)-reboxetine, start inhibiting [^{3}H]cytisine binding to desensitized AChRs at concentrations higher than 100 μM. The apparent IC_{50} values for TCAs are in the ∼0.5–1.5 mM concentration range (see Table 2), indicating that TCAs bind to the agonist binding sites with extremely low affinity. The fact that (−)-reboxetine does not bind to the AChR agonist sites is in agreementwith previous radioligand binding results (Miller et al., 2002).

Table 2
Binding affinity of (−)-reboxetine for the [^{3}H]TCP binding sites and modulation of [^{3}H]cytisine binding to *Torpedo* AChRs by (−)-reboxetine and tricyclic antidepressants.

Antidepressant	Radioligand	Resting/α-BTx-bound state		Desensitized/agonist-bound state	
		K_i (μM) [a]	n_H[d]	K_i (μM)[a]	n_H[d]
(−)-Reboxetine	[^{3}H]TCP	28 ± 2	1.09 ± 0.07	2.2 ± 0.2	1.05 ± 0.09
		Resting but activatable state		Desensitized/proadifen-bound state	
		Apparent EC_{50}[b] (μM)	Apparent n_H[d]	Apparent IC_{50}[c] (mM)	Apparent n_H[d]
(−)-Reboxetine	[^{3}H]Cytisine	1.7 ± 0.4	0.76 ± 0.12	No competition	–
Imipramine		1.2 ± 0.4	0.80 ± 0.16	0.9 ± 0.2	1.78 ± 0.44
Amitriptyline		2.8 ± 0.4	0.96 ± 0.14	1.5 ± 0.4	1.74 ± 0.44
Doxepin		1.8 ± 0.4	0.90 ± 0.14	0.5 ± 0.1	0.84 ± 0.12

[a] K_i values were obtained from Fig. 2, in the presence of α-BTx (resting state) or CCh (desensitized state), according to Eq. (1).
[b] Antidepressant concentration required to enhance 50% [^{3}H]cytisine binding was obtained using AChRs in the resting but activatable state (in the absence of proadifen) (Fig. 3).
[c] Antidepressant concentration required to inhibit 50% [^{3}H]cytisine binding was obtained using AChRs in the desensitized state (in the presence of 200 μM proadifen) (Fig. 3).
[d] Hill coefficient.

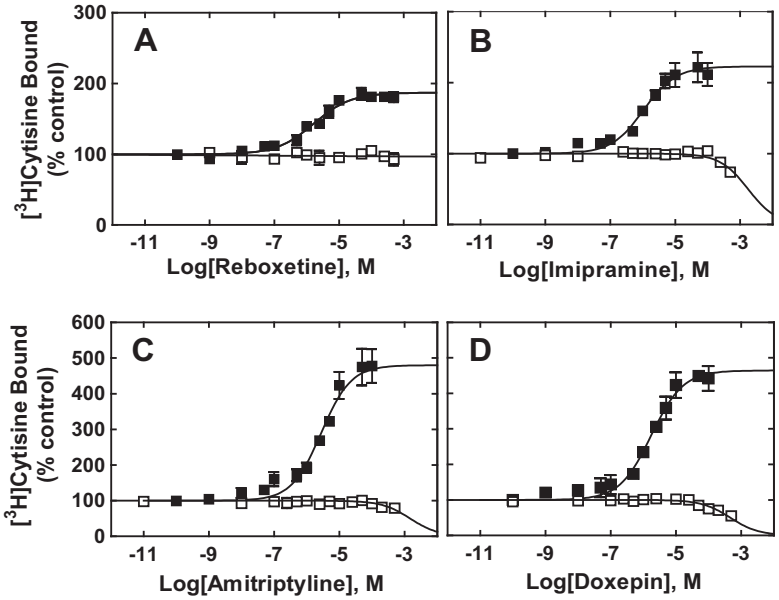

Fig. 3. Modulation of [^{3}H]cytisine binding to *Torpedo* AChRs mediated by (A) (−)-reboxetine, (B) imipramine, (C) amitriptyline, and (D) doxepin. AChR native membranes (0.3 μM) were equilibrated (30 min) with 7.7 nM [^{3}H]cytisine, in the absence (■) (resting but activatable state) or in the presence of 200 μM proadifen (□) (desensitized/proadifen-bound state), and increasing concentrations of the studied antidepressant. Nonspecific binding was determined in the presence of 1 mM CCh. The plots are the combination of two separated experiments each one performed in triplicate, where the error bars represents the S.D. values. The IC_{50}, apparent EC_{50}, and n_H values are summarized in Table 2.

3.3. Molecular docking and molecular dynamics of (−)-reboxetine interacting with muscle AChRs

(−)-Reboxetine docked the *Torpedo* AChR in two qualitative different regions (Fig. 4A; Table 3): a luminal site, overlapping the PCP locus, and three non-luminal sites, each one located at the extracellular end of the transmembrane domain (TMD) from the α1, β1, or γ subunit. Both (−)-reboxetine and PCP conformers make contacts with M2 residues spanning from position 6′ (serine ring) to 14′ (Table 3; Fig. 4A and B), approximately in the middle of the ion channel. Two conformers of (−)-reboxetine (one neutral and one protonated) were found to bind to this region (Table 3). The neutral conformer makes contact with α1-Ser248, β1-Ser254, and δ-Cys262 at the serine ring; α1-Leu251 and δ-Leu265 at the leucine ring (position 9′); α1-Ser252, β1-Ala258, δ-Ala266, and γ-Ala260 at position 10′; and γ-Ile263 and δ-Val269 at the valine ring (position 13′) (Fig. 4B). The protonated conformer also makes contact with γ-Phe264 at position 14′. All ligand–receptor interactions are hydrophobic in nature, with the exception of one of the two α1-Ser248 which makes polar contacts. In the γ-intrasubunit site, (−)-reboxetine interacts with residues from M1 (i.e., Tyr221 and Ile225), M2 (i.e., Val272 at position 22′), M3 (i.e., Tyr285, Leu286, Phe288, and Val289), and M4 (i.e., Thr468), as well as from the extracellular region of the γ-subunit (i.e., Leu219, Phe134, Phe136, and Lys217) (Fig. 4C).

In human adult muscle AChRs, (−)-reboxetine conformers at the β1-intrasubunit and α1/ε intersubunit sites were also found (Table 3; Fig. 5A and B), but surprisingly none in the ion channel lumen. At the β1-intrasubunit site, neutral (−)-reboxetine makes contacts with residues from M2 (i.e., Val261) and M3 (i.e., Pro269, Ile270, Ile271, Tyr274 and Leu275) (Table 3). At the intersubunit site, protonated (−)-reboxetine makes contacts with residues from α1-M2 (i.e., Leu258 at position 16′, Val261 at position 19′, and Glu262 at position 20′, ε-M2 (i.e., Phe266 at position 14′, Leu269 at position 17′, and Ile270 at position 18′), and ε-M1 (i.e., Tyr223, Asn226, and Ile227), and from the extracellular region of the ε-subunit (i.e., Lys273 and Ile274). Although the side chain sidesof Glu262 and Leu269 are oriented to the channel lumen, the ligand is contacted from the TMD interior interface. All interactions are hydrophobic, except a polar interaction with ε-Asn226 and a cation–π interaction with ε-Lys273.

Since a (−)-reboxetine conformer was found overlapping the PCP locus in *Torpedo* AChRs, the stability of (−)-reboxetine in this domain was compared to that for PCP by 10-ns molecular dynamics simulations. Fig. 6A shows that (−)-reboxetine is rapidly stabilized at a RMSD value of 0.3 nm. PCP stabilizes at a value of 0.5 nm but after 5-ns simulation it jumps to a RMSD of 1.2 nm. According to this analysis, (−)-reboxetine, in the luminal site, is more stable than PCP. The predicted affinities of (−)-reboxetine for the non-luminal sites suggest that they are also plausible binding sites (Table 3). Thus, to test the stability of these conformers, 20-ns molecular dynamics simulations were performed (Fig. 6B–D). (−)-Reboxetine within the α1-TMD makes a smaller initial reorientation but remains in its new orientation for short periods, indicating that this pose is less stable (Fig. 6B). The most unstable conformer was that docked within the β1-TMD, which goes from its original position to a new totally different position (Fig. 6C). The most stable pose was that for the γ-intrasubunit site (Fig. 6D). This conformer makes a strong reorientation from its original position, but it stabilizes in this binding domain after 10-ns simulation. Therefore, (−)-reboxetine finds a stable docking position only within the γ-TMD.

3.4. In silico mutations at amino acid rings involved in (−)-reboxetine interaction with Torpedo, human muscle and α4β2 AChR ion channels

To confirm the importance of the amino acid rings involved in the binding of (−)-reboxetine to the *Torpedo* ion channel, Ala-scanning mutagenesis was performed at the serine (position 6′), leucine (position 9′), and valine (position 13′) rings. In a recent work we showed that (−)-reboxetine binds to the hα4β2 AChR ion channel in a site between rings 6′ and 14′ (Arias et al., 2013), therefore a similar experiment was carried out in this receptor. The common critical residue for binding was the leucine ring at position 9′ (Table 4 and Supplementary Material). In all mutations, the calculated K_i values were higher, indicating lower affinity (Table 4).

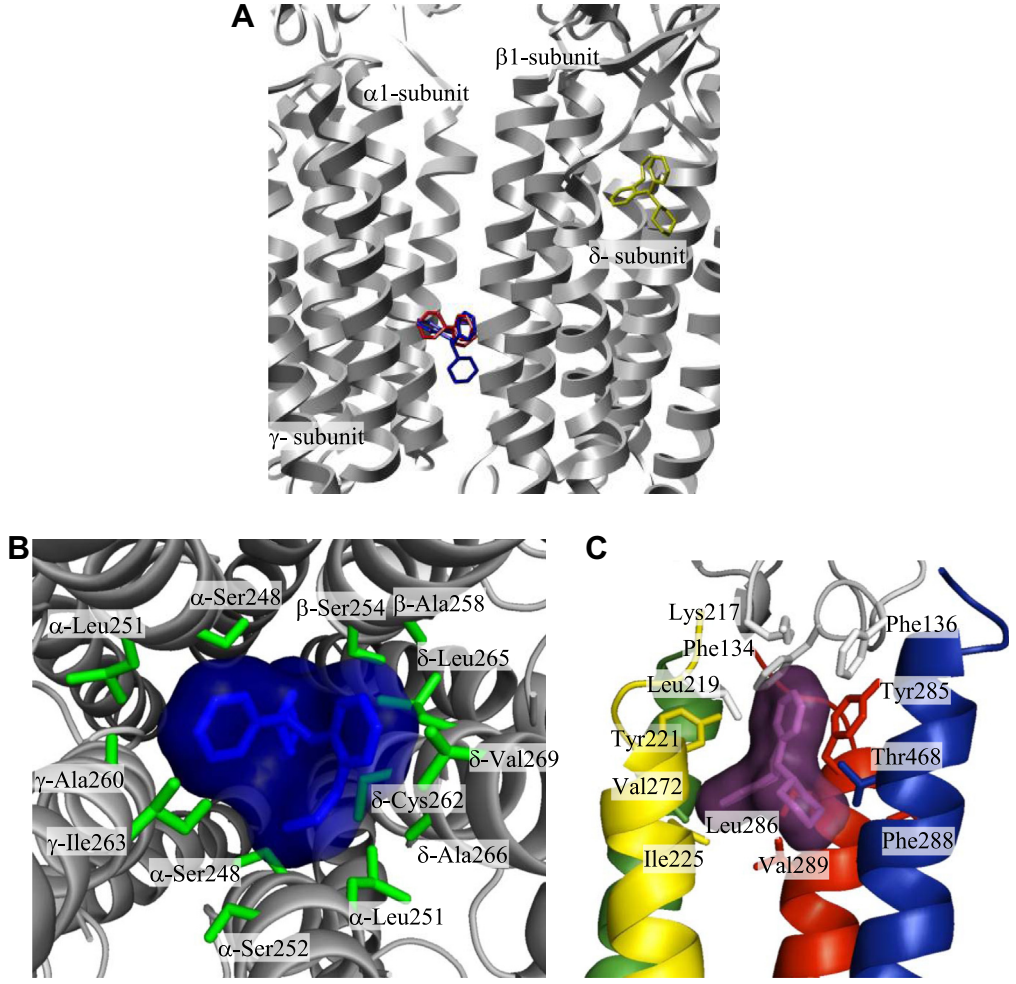

Fig. 4. Most stable docking positions of (−)-reboxetine at the *Torpedo* AChR. (A) View of the most stable docking positions of (−)-reboxetine at the γ-intrasubunit (i.e., non-luminal site) (yellow) and luminal site (blue). Both PCP (red) and (−)-reboxetine (blue) structures are superposed, demonstrating overlapping sites. (B) Detailed view of the luminal binding site for neutral (−)-reboxetine. The residues that interact with (−)-reboxetine are α1-Ser248, α1-Leu251, α1-Ser252, β1-Ser254, β1-Ala258, γ-Ala260, γ-Ile263, δ-Cys262, δ-Leu265, δ-Ala266, and δ-Val269. Ligand–receptor interactions in this site are hydrophobic, except for one of the two α1-Ser248 which makes polar contacts. (C) Detailed view of the γ-intrasubunit site for (−)-reboxetine (magenta) [see conformer in yellow in panel (A)]. Residues belong to M1 (yellow) (i.e., Leu 219, Tyr221 and Ile225), M2 (green) (i.e., Val272), M3 (red) (i.e., Tyr285, Leu286,Phe288, and Val289), and M4 (blue) (i.e., Thr468), and to the extracellular region (white) (i.e., Phe134, Phe136, and Lys217) of the γ-subunit. (For interpretation of the references to colour in this figure legend, the reader is referred to the web version of this article.)

Table 3
Residues involved in the binding of (−)-reboxetine to the transmembrane domain of the *Torpedo* and human muscle AChRs and the corresponding theoretical binding affinities.

Receptor Domain	Reboxetine state	M1	M2															M3	M4	Total	K_i(μM)
			L 6′	NL 7′	L 9′	NL 10′	NL 12′	L 13′	NL 14′	NL 15′	NL 16′	L 17′	NL 18′	NL 19′	L 20′	NL 21′	NL 22′				
Torpedo																					
Non-luminal domain																					
α1-TMD	N	5																3	4	12	1.1
	P	2															1	6		9	1.6
β1-TMD	N	3															1	5		9	1.9
	P	3															1	5		9	1.9
γ-TMD	N	3															1	4		8	0.3
	P	3															1	4		8	0.3
Luminal domain																					
	N		1		2	3		2												8	1.6
	P		2		2	3		4	2											13	1.6
Human Muscle																					
α1/ε-TMD interface	P	4							1		1	1	1	1	1	1	1			12	0.6
β1-TMD	N	6															1	5		6	0.5

For the transmembrane segments M1, M3, and M4, the total number of different residues involved in the binding of (−)-reboxetine is represented.
For the transmembrane segment M2, the relative position of the residue within this segment and whether it is luminal (L) or non-luminal (NL) is shown.
N and P, neutral and protonated state, respectively.

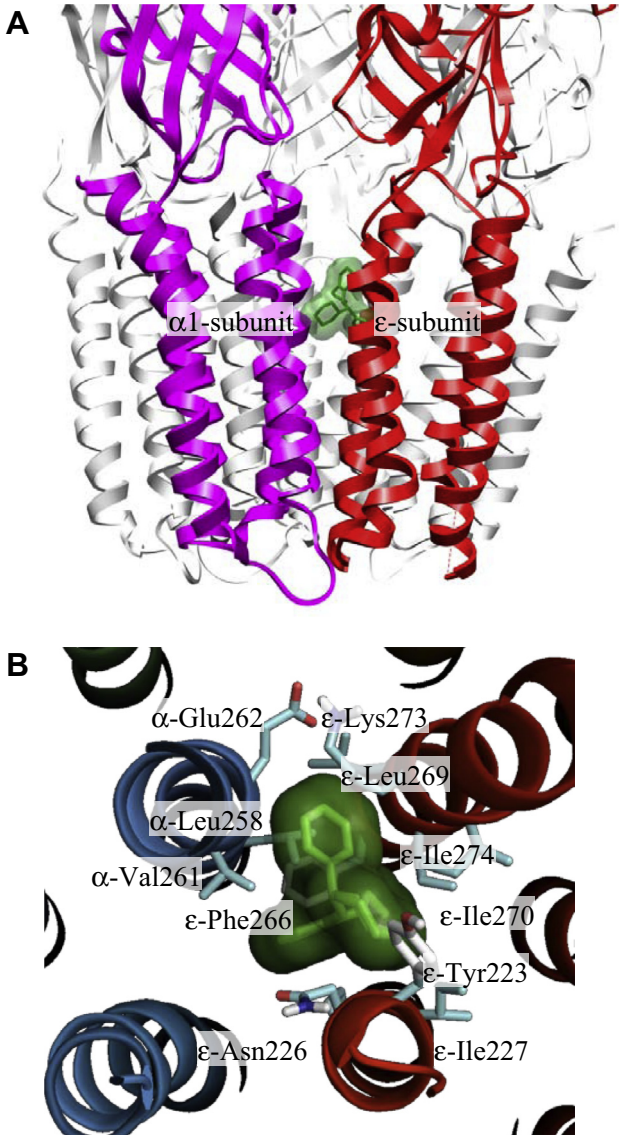

Fig. 5. Most stable docking positions of (−)-reboxetine at the human adult muscle AChR. (A) View of the extracellular portion of the human adult muscle AChR showing the most stable docking position of (−)-reboxetine at the α1 magenta ribbon) and ε (red ribbon) subunit interface (i.e., non-luminal site). (B) Detailed view of the α1/ε-intersubunit site for (−)-reboxetine. The residues at the α1-M2 segment (blue ribbon) are Leu258 (position 16′), Val261 (position 19′), and Glu262 (ring 20′), whereas the residues at the ε-M2 segment (red ribbon) are Phe266 (position 14′), Leu269 (position 17′), and Ile270 (position 18′). In addition, the residues from the ε-M1 segment are Tyr223, Asn226, and Ile227, and the residues from the extracellular region of the ε-subunit are Lys273 and Ile274. All these interactions are hydrophobic in nature, except the polar interaction with ε-Asn226, and the cation–π interaction with ε-Lys273. (For interpretation of the references to colour in this figure legend, the reader is referred to the web version of this article.)

Thisvalidates the docking in the wild-type receptor and the importance of the leucine ring in the binding of (−)-reboxetine. *In silico* mutations were also performed in order to explain the differences in the binding of (−)-reboxetine to *Torpedo* and muscle receptors, however no strong conclusions were obtained in this regard (see details in Supplementary Material).

4. Discussion

The (±)-epibatidine-activated Ca^{2+} influx results indicate that (±)-epibatidine is ∼2-fold more potent activating the hα1β1γδ (embryonic) AChR compared to the hα1β1εδ (adult) muscle AChR (see Table 1). A potential explanation is that (±)-epibatidine binds to the embryonic AChR with ∼2-fold higher affinity than that for the adult AChR (Prince and Sine, 1999), and/or that (±)-epibatidine is a more potent blocker (i.e., self-blocking mechanism) of the hα1β1εδ AChR ion channel compared to the hα1β1γδ AChR ion channel (Prince and Sine, 1998). In addition, the observed n_H values (see Table 1) suggest that (±)-epibatidine can discriminate between both agonist binding sites at the adult muscle AChR better-than that at the embryonic AChR.

The (−)-reboxetine inhibitory potency for the hα1β1εδ AChR (embryonic) is ∼2-fold higher than that for the hα1β1γδ AChR (adult) subtype (see Table 1). Since this inhibition is mediated by a non-competitive mechanism (Fig. 1C), and considering that [^{3}H]TCP binds to the AChR ion channel (Arias et al., 2003, 2006), we tested the hypothesis that (−)-reboxetine binds to the *Torpedo* AChR lumen by [^{3}H]TCP competition binding experiments. The results indicate that in fact (−)-reboxetine binds to the [^{3}H]TCP site in a steric fashion ($n_H \sim 1$), and that its affinity for the desensitized AChR is ∼13-fold higher than that for theresting AChR (see Table 2). This luminal interaction agrees with the non-competitive mechanism of inhibition elicited by (−)-reboxetine (see Fig. 1C).

The [^{3}H]cytisine binding results indicate that (−)-reboxetine and TCAs enhance [^{3}H]cytisine binding (see Fig. 3A), suggesting that these structurally different antidepressants induce AChR desensitization. Our results support the idea that the pharmacological action of (−)-reboxetine and TCAs is not mediated by just one mechanism but by a combination of non-competitive inhibitory and desensitizing mechanisms. A similar conclusion was obtained for (−)-reboxetine-induced inhibition of hα4β2 AChRs (Arias et al., 2013). The combination of blocking and desensitizing mechanisms was previously determined for TCAs, bupropion and its derivatives, and serotonin selective reuptake inhibitors in muscle- (Arias et al., 2009, 2010a; Gumilar et al., 2003; López-Valdés et al., 2001) and neuronal-type AChRs (Arias et al., 2010b–d; Gumilar and Bouzat, 2008; López-Valdés and García-Colunga, 2001). This evidence suggests that there is a basic mechanistic motif for structurally different antidepressants underlying the non-competitive inhibition of AChRs.

Previous results from our laboratory indicate that PCP and TCAs (Gumilar and Bouzat, 2008; Sanghvi et al., 2008), serotonin selective reuptake inhibitors (Arias et al., 2010a), and bupropion and its derivatives (Arias et al., 2009), bind to overlapping sites in a domain formed between the threonine (position 2′) and valine (position 13′) rings in the *Torpedo* AChR ion channel. In this regard, our radioligand binding (Table 2), docking (Fig. 4A and C), and *in silico* mutation (Table 4 and Supplementary Material) results support the view that(−)-reboxetine also binds to the same binding domain as that for PCP/TCP in the *Torpedo* AChR ion channel, indicating that there is an overlapping binding site for structurally different non-competitive antagonists. Interestingly, comparison of the *in silico* Ala-scanning mutations between the *Torpedo* and hα4β2 AChRs (Table 4) suggests that the leucine ring is the minimum structural component for (−)-reboxetine. This result is important for the planning of adequate mutation experiments to test this hypothesis.

Docking results support the view that (−)-reboxetine inhibits the *Torpedo* AChR ion channel by a steric blocking mechanism (Fig. 4B). In addition, (−)-reboxetine favors desensitization, maybe by interacting with the γ-intrasubunit site. In the hα4β2 AChR we found a similar behavior, but in this case (−)-reboxetine interacts within the α4-TMD (Arias et al., 2013). Interestingly, (−)-reboxetine binds to the human adult muscle AChR in a different way, by interacting with an intersubunit site formed by the α1 and ε-TMDs. This conformer position does not block the channel directly, but considering that the human adult muscle channel is smaller

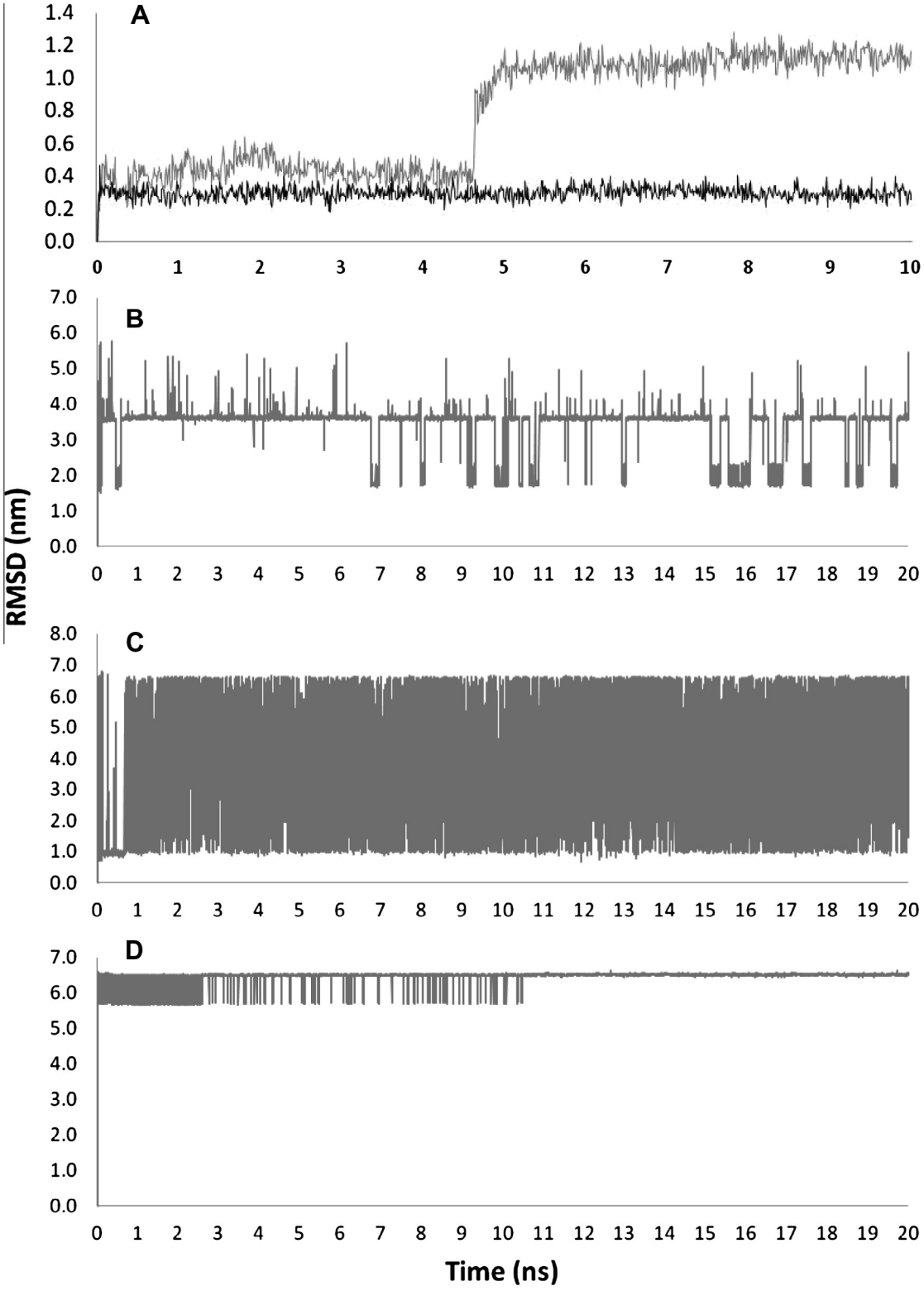

Fig. 6. RMSDA plots obtained from the molecular dynamics simulations performed in the *Torpedo* AChR. (A) 10-ns simulation of PCP (grey line) and (−)-reboxetine (black line). 20-ns simulation of neutral (−)-reboxetine within the α1-(B), β1-(C), and γ-TMD (D), respectively. Only the interaction with the γ-intrasubunit site (D) is stable.

than that for the *Torpedo* AChR (see Supplementary Material), this interaction might suffice to hinderion flux. If AChR desensitization is an important aspect of the (−)-reboxetine pharmacological action (see Table 2; and Arias et al., 2013), the observed non-luminal sites in the *Torpedo*, human adult muscle (see Figs. 4 and 5), and hα4β2 (Arias et al., 2013) AChRs might play important roles on this respect. The characterization of non-luminal sites presents a challenge because we do not have specific probes that can be used to

Table 4
Effect of*in silico* mutations of residues involved in (−)-reboxetine binding to the hα1β1εδ, *Torpedo*, and hα4β2 AChRs.

Ring	hα1β1εδ AChR (adult)		*Torpedo* AChR (α1β1γδ; embryonic)		hα4β2 AChR	
	Wild type	Single mutations at ring 6′: ε-Asn258Ser, and/or β1-Phe245Ser, and/or δ-Ser247Cys	Wild type	Ala-scanning mutation	Wild type	Ala-scanning mutation
6′	No binding	No binding	K_i = 1.6	K_i = 2.3	K_i = 0.6	K_i = 1.0
9′				No binding		No binding
13′				K_i = 3.2		No binding

K_i, emulated binding affinities are in μM.
"No binding" indicates that no conformers were found within the ion-channel in the docking experiments.

pin point these sites. In this regard, other approaches, including site directed mutagenesis, can be used to address this question.

In conclusion, (−)-reboxetine blocks muscle AChRs by direct interaction with the PCP luminal site, and induces receptor desensitization probably by binding at other non-luminal sites, mechanisms that are shared with TCAs.

Acknowledgements

This research was supported by a grant from the Consejo Nacional de Investigaciones Científicas y Técnicas (CONICET; Argentina) (to M.O.O.). The authors thank to National Institute on Drug Addiction (NIDA, NIH, Bethesda, Maryland, USA) for its gift of phencyclidine.

Appendix A. Supplementary data

Supplementary data associated with this article can be found, in the online version, at http://dx.doi.org/10.1016/j.neuint.2013.07.009.

References

Andreasen, J.T., Redrobe, J.P., 2009. Nicotine, but not mecamylamine, enhances antidepressant-like effects of citalopram and reboxetine in the mouse forced swim and tail suspension tests. Behav. Brain Res. 197, 150–156.
Andreasen, J.T., Nielsen, E.Ø., Christensen, J.K., Olsen, G.M., Peters, D., Mirza, N.R., Redrobe, J.P., 2011. Subtype-selective nicotinic acetylcholine receptor agonists enhance the responsiveness to citalopram and reboxetine in the mouse forced swim test. J. Psychopharmacol. (London, UK) 25, 1347–1356.
Arcava, Y., Albuquerque, E.X., 1984. Meproadifen enhances activation and desensitization of the acetylcholine receptor-ionic channel complex (AChR): single channel studies. FEBS Lett. 174, 267–274.
Arias, H.R., Trudell, J.R., Bayer, E.Z., Hester, B., McCardy, E.A., 2003. Noncompetitive antagonist binding sites in the *Torpedo* nicotinic acetylcholine receptor ion channel. Biochemistry 42, 7358–7370.
Arias, H.R., Bhumireddy, P., Bouzat, C., 2006. Molecular mechanisms and binding site locations for noncompetitive antagonists of nicotinic acetylcholine receptors. Int. J. Biochem. Cell Biol. 38, 1254–1276.
Arias, H.R., Gumilar, F., Rosenberg, A., Targowska-Duda, K.M., Feuerbach, D., Jozwiak, K., Moaddel, R., Weiner, I.W., Bouzat, C., 2009. Interaction of bupropion with muscle-type nicotinic acetylcholine receptors in different conformational states. Biochemistry 48, 4506–4518.
Arias, H.R., Feuerbach, D., Bhumireddy, P., Ortells, M.O., 2010a. Inhibitory mechanisms and binding site location for serotonin selective reuptake inhibitors on nicotinic acetylcholine receptors. Int. J. Biochem. Cell Biol. 42, 712–724.
Arias, H.R., Feuerbach, D., Targowska-Duda, K.M., Russell, M.M., Jozwiak, K., 2010b. Interaction of serotonin selective reuptake inhibitors with neuronal nicotinic acetylcholine receptors in different conformational states. Biochemistry 49, 5734–5742.
Arias, H.R., Rosenberg, A., Targowska-Duda, K.M., Feuerbach, D., Jozwiak, K., Moaddel, R., Weiner, I.W., 2010c. Tricyclic antidepressants and mecamylamine bind to different sites in the human α4β2 nicotinic receptor ion channel. Int. J. Biochem. Cell Biol. 42, 1007–1018.
Arias, H.R., Targowska-Duda, K.M., Sullivan, C.J., Feuerbach, D., Maciejewski, R., Jozwiak, K., 2010d. Different interaction between tricyclic antidepressants and mecamylamine with the human α3ß4 nicotinic acetylcholine receptor. Neurochem. Int. 56, 642–649.
Arias, H.R., Fedorov, N.B., Benson, L.C., Lippiello, P.M., Gatto, G.J., Feuerbach, D., Ortells, M.O., 2013. Functional and structural interaction of (−)-reboxetine with the human α4β2 nicotinic acetylcholine receptor. J. Pharmacol. Exp. Ther. 344, 113–123.
Brooks, B.R., Bruccoleri, R.E., Olafson, B.D., States, D.J., Swaminathan, S., Karplus, M., 1983. CHARMM: a program for macromolecular energy, minimization, and dynamics calculations. J. Comput. Chem. 4, 187–217.
Cheng, Y., Prusoff, W.H., 1973. Relationship between the inhibition constant (K_i) and the concentration of inhibitor which causes 50 percent inhibition (IC_{50}) of an enzymatic reaction. Biochem. Pharmacol. 22, 3099–3108.
Grubmueller, H., 1996. SOLVATE v. 1.0. Theoretical Biophysics Group, Institute for Medical Optics, Ludwig-Maximilians University, Munich.
Gumilar, F., Bouzat, C., 2008. Tricyclic antidepressant inhibit homomeric Cys-Loop receptors by acting at different conformational states. Eur. J. Pharmacol. 584, 30–39.
Gumilar, F., Arias, H.R., Spitzmaul, G., Bouzat, C., 2003. Molecular mechanism of inhibition of nicotinic acetylcholine receptors by tricyclic antidepressants. Neuropharmacology 45, 964–976.
Keserü, G., Kolossváry, I., 1999. Molecular mechanics and conformational analysis in drug designlackwell Science Ltd. UK, Oxford.
López-Valdés, H.E., García-Colunga, J., 2001. Antagonism of nicotinic acetylcholine receptors by inhibitors of monoamine uptake. Mol. Psychiatr. 6, 511–519.
Mathur, A., Shankaracharya Vidyarthi, A.S., 2011. SWIFT modeller: a Java based GUI for molecular modeling. J. Mol. Model. 17, 2601–2607.
Michelmore, S., Croskery, K., Nozulak, J., Hoyer, D., Longato, R., Weber, A., Bouhelal, R., Feuerbach, D., 2002. Study of the calcium dynamics of the human α4β2, α3β4 and α1β1γδ nicotinic acetylcholine receptors. Naunyn-Schmiedebergs Arch. Pharmacol. 366, 235–245.
Miller, D.K., Erik, H.F., Wong, M., Chesnut, M.D., Dwoskin, L.P., 2002. Reboxetine: functional inhibition of monoamine transporters and nicotinic acetylcholine receptors. J. Pharmacol. Exp. Ther. 302, 687–695.
Miyazawa, A., Fujiyoshi, Y., Unwin, N., 2003. Structure and gating mechanism of the acetylcholine receptor pore. Nature 423, 945–949.
Moore, M.A., McCarthy, M.P., 2012. Snake venom toxins, unlike smaller antagonists, appear to stabilize a resting state conformation of the nicotinic acetylcholine receptor. Biochim. Biophys. Acta 1235, 336–342.
Öhman, D., Cherma, M.D., Norlander, B., Bengtsson, F., 2003. Determination of serum reboxetine enantiomers in patients on chronic medication with racemic reboxetine. Ther. Drug. Monit. 25, 174–182.
Pagán, O.R., Eterovic, V.A., García, M., Vergne, D., Basilio, C.M., Rodríguez, A.D., Hann, R.M., 2001. Cembranoid and long-chain alkanol sites on the nicotinic acetylcholine receptor and their allosteric interaction. Biochemistry 40, 11121–11130.
Pedretti, A., Villa, L., Vistoli, G., 2004. VEGA – an open platform to develop chemo-bio-informatics applications, using plug-in architecture and script programming. J. Comput. Aided Mol. Des. 18, 167–173.
Phillips, J.C., Braun, R., Wang, W., Gumbart, J., Tajkhorshid, E., Villa, E., Chipot, C., Skeel, R.D., Kale, L., Schulten, K., 2005. Scalable molecular dynamics with NAMD. J. Comput. Chem. 26, 1781–1802.
Prince, R.J., Sine, S.M., 1998. Epibatidine activates muscle acetylcholine receptors with unique site selectivity. Biophys. J. 75, 1817–1827.
Prince, R.J., Sine, S.M., 1999. Acetylcholine and epibatidine binding to muscle acetylcholine receptors distinguish between concerted and uncoupled models. J. Biol. Chem. 274, 19623–19629.
Rauhut, A.S., Mullins, S.N., Dwoskin, L.P., Bardo, M.T., 2002. Reboxetine: attenuation of intravenous nicotine self-administration in rats. J. Pharmacol. Exp. Ther. 303, 604–672.
Šali, A., Blundell, T.L., 1993. Comparative protein modelling by satisfaction of spatial restraints. J. Mol. Biol. 234, 779–815.
Sanghvi, M., Hamouda, A.K., Jozwiak, K., Blanton, M.P., Trudell, J.R., Arias, H.R., 2008. Identifying the binding site(s) for antidepressants on the *Torpedo* nicotinic acetylcholine receptor: [^{3}H]2-Azidoimipramine photolabeling and molecular dynamics studies. Biochim. Biophys. Acta 1778, 2690–2699.
Trott, O., Olson, A.J., 2010. AutoDock Vina: improving the speed and accuracy of docking with a new scoring function, efficient optimization and multithreading. J. Comput. Chem. 31, 455–461.
Unwin, N., 2005. Refined structure of the nicotinic acetylcholine receptor at 4 Å resolution. J. Mol. Biol. 346, 967–989.